Bacteriorhodopsin Analog Regenerated with 13-Desmethyl-13-Iodoretinal

Kenji Hiraki,* Toshiaki Hamanaka,† Xiang-Guo Zheng,* Teturo Shinada,* Jong-Moon Kim,* Kazuo Yoshihara,* and Yuji Kito‡

*Suntory Institute for Bioorganic Research, Wakayamadai, Shimamoto, Osaka 618-0024, Japan; †Department of Systems and Human Science, Graduate School of Engineering Science, Osaka University, Toyonaka, Osaka 560-8531, Japan; and ‡TYK Laboratory for Photobiology, Yokata, Toyama 930-2243, Japan

ABSTRACT The retinal analog 13-desmethyl-13-iodoretinal (13-iodoretinal) was newly synthesized and incorporated into apomembranes to reconstitute bacteriorhodopsin analog 13-I-bR. The absorption maximum was 598 nm and 97% of the chromophore was an all-*trans* isomer in the dark- and light-adapted state. Upon flash illumination, 13-I-bR underwent a transient spectral change in which a shorter wavelength intermediate (λ_{max} = 426 nm) similar to the M species of the native bR developed. Also, 13-I-bR showed light-induced proton pumping with rates and extents comparable to those seen in the native bR. The ultraviolet circular dichroism (CD) spectrum originating from the aromatic groups was different from that of the native bR, indicating that the substituted bulky iodine atom strongly interacts with neighboring amino acids. A projection difference Fourier map showed the labeled iodine was in the vicinity of helix C. 13-I-bR is an advantageous specimen for kinetic investigations of light-induced structural changes associated with the proton pumping cycle by x-ray diffraction.

INTRODUCTION

Bacteriorhodopsin (bR) is a seven-helix membrane protein, which functions as a light-driven proton pump. The bR molecule is a chromoprotein that consists of bacterioopsin (bO), a 26-kDa protein, and the chromophore retinal. Retinal is covalently attached to the protein moiety through a protonated Schiff base linkage to the ϵ-amino group of Lys-216 (Oesterhelt and Stoeckenius, 1974; Stoeckenius and Bogomolni, 1982).

To elucidate the molecular mechanism of the vectorial proton translocation associated with the photocycle of bR, many studies have been performed (for reviews, see Oesterhelt et al., 1992; Ebrey, 1993; Lanyi, 1993). Upon photon absorption, the photoisomerization of retinal from an all-*trans* to a 13-*cis* isomer triggers a cyclic photochemical reaction that involves a series of intermediates referred to as J, K, L, M, N, and O. Before and after the formation of the M intermediate, one proton is translocated from the cytoplasmic to the extracellular side.

The molecular structure of bR has been determined by electron cryomicroscopy studies (Grigorieff et al., 1996; Kimura et al., 1997) and x-ray crystallography (Pebay-Peyroula et al., 1997; Luecke et al., 1999a). In addition, all-atom descriptions, including interhelical loops that are perturbed in positions and cannot be determined with sufficient accuracy by diffraction methods, have been estimated by molecular dynamic simulations (Humphrey et al., 1994). The light-induced structural changes of photointermediates trapped at low temperature have been explored by x-ray crystallography (Luecke et al., 1999b; Edman et al., 1999; Sass et al., 2000; Royant et al., 2000) and by electron microscopy (Subramaniam and Henderson, 2000).

Retinal directly participates in vectorial proton pumping via a protonated Schiff base linkage (Govindjee et al., 1988). In the chromophore pocket, the steric interactions between the 9-methyl and the 13-methyl group of the chromophore and the neighboring amino acid residues are essential for the bR function (Weidlich et al., 1996; Gärtner et al., 1983). Subramaniam et al. (1999) proposed that the subtle structural rearrangements triggered by light absorption in retinal and/or the protein were important for the molecular switch from the L state to the M2 state in the bR photocycle. The pigment containing the retinal analog labeled with a heavy atom will be useful in understanding the stereodynamics of the retinal molecule during the photocycle by x-ray kinetic experiments.

Büldt et al. (1991) have prepared the bR analogs regenerated with 9-bromoretinal or 13-bromoretinal, in which the methyl group bound to C-9 or C-13 of the polyene chain is replaced by a bromine atom, and determined the labeled sites of bromine on the projection density map normal to the membrane plane based on the x-ray diffraction data. Bromine is a rather weak label as a heavy atom. If the retinal analog labeled with a heavy atom containing more electrons than bromine is available, the change of x-ray diffraction intensity becomes larger and a label location on the difference Fourier density map will be definitely determined.

In this study, the iodine-substituted retinal analog (13-iodoretinal, Fig. 1) in which the methyl group bound to C-13 of retinal was replaced by iodine, was newly synthesized. The bR analog (13-I-bR) was regenerated with 13-iodoretinal. The all-*trans* isomer was 97% in chromophore composition of the dark-adapted 13-I-bR. 13-I-bR, however, was confirmed to change from an all-*trans* form to a 13-*cis* form upon light illumination and was active in proton

Submitted November 20, 2001, and accepted for publication August 2, 2002.

Address reprint requests to Toshiaki Hamanaka, Department of Systems and Human Science, Graduate School of Engineering Science, Osaka University, Toyonaka, Osaka 560-8531, Japan. Tel.: 06-6850-6516; Fax: 06-6850-6557; E-mail: hamanaka@bpe.es.osaka-u.ac.jp.

0006-3495/02/12/3460/10 $2.00

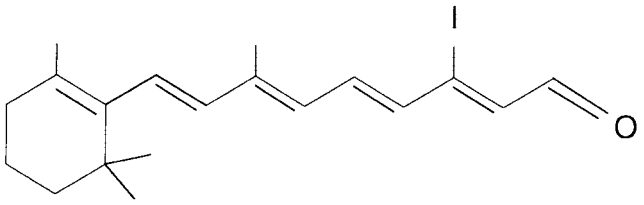

FIGURE 1 All-*trans* 13-iodoretinal.

pumping. In the ultraviolet circular dichroism (CD) spectrum of 13-I-bR, the signals attributable to the aromatic groups in the chromophore pocket changed from that of the native bR. This suggests that the labeled iodine atom interacts strongly with the aromatic groups, such as Trp-182 and Trp-86.

The location of the iodine label was determined on the projection difference density map calculated from difference x-ray diffraction amplitudes with phase angles of electron microscopy studies (Henderson et al., 1986). In the difference density map, the broadening of the main peak and several subpeaks above average noise level were observed. The origins of these were investigated by model calculations, and it was elucidated that neglecting the changes in phase angles of a structure factor inherent in a heavy atom substitution was the main cause.

MATERIALS AND METHODS

Sample preparation

Isolation of purple membrane (PM) was performed according to the method of Oesterhelt and Stoeckenius (1974). Bleached membranes, apomembranes, were prepared by hydroxylamine treatment (pH 7.4) under illumination, followed by repetitive washing with albumin solution to remove retinaloximes (Katre et al., 1981; Hiraki et al., 1987).

The procedure of 13-iodoretinal synthesis will be published elsewhere. Reconstitution of 13-I-bR was carried out by successive addition of microliter quantities of all-*trans* or 13-*cis* of 13-iodoretinal dissolved in ethanol to apomembranes in the dark at room temperature. The final concentration of ethanol was $<1\%$. The reconstituted membrane with 13-iodoretinal is termed 13-I-PM, and that with normal retinal as R-PM.

To investigate the light-dark adaptation, 13-I-PM suspended in 20 mM bis-Tris-HCl (pH 6.5)/100 mM KCl was illuminated ($\lambda > 560$ nm) in a cuvette. Immediately after turning off the light, the absorption spectrum was recorded with a JASCO V-560 spectrophotometer (Nihon Bunkou Co. Ltd., Tokyo, Japan).

CD spectra were recorded with a JASCO J-725 spectropolarimeter (Nihon Bunko Co. Ltd.). The specimen was suspended in 20 mM bis-Tris-HCl (pH 6.5)/100 mM KCl. The light path length was 1 cm or 1 mm.

Chromophores of the dark-adapted pigments or the illuminated one under continuous light ($\lambda > 560$ nm, 2 min) were extracted as aldehyde forms according to the method of Suzuki et al. (1986). Extracted chromophores were analyzed by HPLC equipped with Zorbax SIL column (4.6 × 250 mm, Dupont Co. Ltd.). The mobile phase ratio for hexane/ethyl acetate was 97.5:2.5 (v/v) and the flow rate was 1 ml/min. The absorbance of the eluate was monitored at 390 nm.

To investigate whether the chromophore isomerization occurs during the photocycle, 13-I-bR was illuminated at −74°C and the chromophore was extracted at −40°C; 0.3 mg 13-I-bR was suspended in 100 μl water, and then 200 μl of 0.5 M carbonate buffer (pH 9.5) and 500 μl glycerol were added. The sample in the test tube was stored in dry ice-methanol (−74°C) and illuminated through an R60 filter (600 nm) for ~10 min. Then, the test tube containing the specimen was immersed in the methanol-water bath kept at −40°C with Cryostat (Cryocool CC-100, Portsmouth, NH) and 1 ml dichloromethane, previously cooled at −40°C, was added and homogenized. After the addition of hexane cooled at −40°C, the homogenized specimen was centrifuged at room temperature and the supernatant was analyzed by HPLC.

Flash photolysis

The transient absorption spectra induced in 13-I-bR or the native bR were recorded by 1-ms time slices after flash illumination ($\lambda = 532$ nm, pulse width 5 ns) in the wavelength range of 350–750 nm. Each specimen was suspended in a 20 mM bis-Tris-HCl/100 mM KCl solution (pH 6.5). The temperature of the specimen was controlled at 25°C.

Time courses of M formation and decay were measured at 420 nm for both 13-I-bR and the native bR at 20 or 25°C. The measurement was performed at time scales ranging from 0 to 475 μs for M formation and from 0 to 19 ms for M decay.

The formation and decay of the O intermediate were measured at 710 nm for 13-I-bR and at 660 nm for the native bR or the bR regenerated with normal retinal (R-bR). The time course of recovery to the ground state was monitored at 570 nm for 13-I-bR and at 550 nm for the native bR or R-bR. These measurements were performed at time scales ranging from 0 to 19 ms at 20°C. Each specimen was suspended in 20 mM Tris-HCl/100 mM KCl solution (pH 6.5).

Light-induced pH change

To investigate the proton pump activity of 13-I-bR, the light-induced pH change of the membrane suspensions or the vesicle suspensions was measured. The pH change of the membrane suspension was monitored at pH 6.5 and 6.8 with the optical pH-indicator pyranine (8-hydroxy-1,3,6-pyrenetrisulfonic acid, trisodium salt) according to the literature (Grzesiek and Dencher, 1986; Dencher et al., 1986; Cao et al., 1993). Briefly, each specimen was suspended in 100 mM KCl solution and the pyranine final concentration was ~84 μM in the assay mixture. The pH of the specimens was adjusted to 6.5 or 6.8 by addition of NaOH or HCl, and the time course of the absorbance change was measured at 457 nm. Next, bis-Tris-HCl buffer, pH 6.5 or 6.8, was added in the final concentration of 5 mM and the absorbance change was measured again. The net proton pump activity was determined from the difference between the absorbance changes before and after addition of the buffer. Measurements were performed at 25°C.

Transient absorbance changes were measured with a UNISOKU TSP-601 time-resolved spectrophotometer. The actinic light was the 532-nm, 5-ns, 20 mJ pulse of Q-switched Nd:YAG laser (Surelite I-10: Continuum).

Preparation of vesicles containing 13-I-bR was performed according to the literature (Racker et al., 1979). Light-induced pH change of the vesicle suspension was monitored using a pH meter (M-12, Horiba) equipped with a pH electrode (6378–10D, Horiba). Before illumination, the pH of suspensions was adjusted to ~6.5 with NaOH or HCl.

X-ray diffraction

In x-ray experiments, oriented or nonoriented membrane specimens were used. Nonoriented specimens were prepared as follows. Native PM or 13-I-PM suspended in 20 mM bis-Tris-HCl/5 mM KCl solution (pH 6.5) was centrifuged at 30,000 rpm for 30 min. The pellet was diluted to ~40 optical density and sealed in a glass capillary (1 mm diameter). The x-ray diffraction patterns of these specimens were isotropic powder ones. Oriented specimens, membrane films, were prepared by drying the membrane

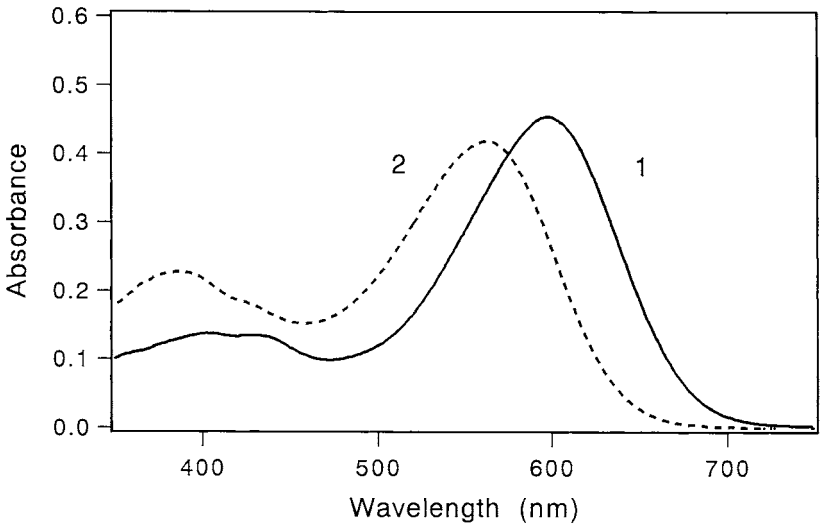

FIGURE 2 Absorption spectra of 13-I-bR (1) and the native bR (2).

pellet placed on 10-μm-thick aluminum foil at a relative humidity of 95% (Hamanaka et al., 1982).

The source was a fine-focus rotating anode x-ray generator, a Rigaku RU-100 unit (Rigaku Denki Co. Ltd.), and run at 40 kV and 25 mA. The monochromatized CuKα_1 ($\lambda = 0.15405$ nm) beam was focused by mirror and monochromator (camera length 18 cm). The x-ray diffraction pattern was recorded on an imaging plate (Fuji Photo Film Co. Ltd.). After exposure, x-ray intensity was read by an image scanner (BAS2000, Fuji Photo Film Co. Ltd.).

The integrated intensities of powder diffraction lines were obtained after subtraction of the background level and Lorentz correction. Lorentz correction was performed by comparing the diffraction intensity of the oriented specimen with that of the nonoriented specimen, according to Eq. 1. The parameter n in the equation was determined by least-squares.

$$I_{no}(s) = I_{or}(s) \times s^n \tag{1}$$

where $I_{no}(s)$ is the diffraction intensity of the nonoriented specimen corrected by s^2, $I_{or}(s)$ is the observed intensity of the oriented specimen, s^n is the Lorentz factor of the oriented specimen, $s = 2\sin(\theta)/\lambda$, 2θ is the diffraction angle, and λ is the wavelength of incident x-ray beam.

Several nonequivalent reflections overlapped in a powder line due to the same value of $h^2 + hk + k^2$, such as (h, k) and (k, h) reflections, were separated using the intensity ratios based on electron microscopy studies (Henderson et al., 1986). The integrated intensities of (1, 0), (3, 0), (3, 3), (6, 0), and (4, 4) reflections were set to 0.

Diffraction intensity of 13-I-PM and native PM were scaled as follows. The ratios of the observed x-ray intensities to the calculated intensities from atomic coordinates of bR in the Brookhaven Protein Data Bank (identification code 2BRD) were compared for each (h, k) reflection. The ratios in the region ranging from (3, 1) to (7, 1) reflections showed almost uniform distribution around an average value. Multiplying each intensity by this average ratio, both data were scaled.

Structure factor amplitude was derived for each reflection as the square root of the scaled integrated intensity. Difference amplitudes were combined with phase angles from electron microscopic studies (Henderson et al., 1986) to yield a projection difference density map to an 0.7 nm resolution.

The location of the iodine label was refined according to the procedure described by Jubb et al. (1984). Briefly, the area shown in Fig. 7 *A* was divided into 90×90 grids. The structure factor of the iodine-labeled PM model was constructed by combining the structure factor of the native PM with that of iodine placed at one of the above sections. Diffraction intensity of this model was calculated according to Eq. 2.

$$I_c^I(h, k) = |F_{nat}(h, k) + a \times F_I(h, k)|^2 \tag{2}$$

where $F_{nat}(h, k)$ is the structure factor of the native PM, $F_I(h, k)$ is the structure factor of iodine positioned at one of the sections, and the parameter a is the scale factor, denoting the occupancy. The R factor to be minimized is:

$$R = \Sigma(I_o^I(h, k) - b \times I_c^I(h, k))^2/\Sigma(I_o^I(h, k) - I_o^N(h, k))^2 \tag{3}$$

where $I_o^I(h, k)$ is the observed intensity of 13-I-PM, $I_o^N(h, k)$ is the observed intensity of the native PM, $I_c^I(h, k)$ is the intensity calculated from an iodine-labeled PM model (Eq. 2), and b is the scale factor (Jubb et al., 1984). The label position was moved over these sections and the position where the calculated R value (Eq. 3) became minimum was searched.

RESULTS

Dark-adapted 13-I-bR

The absorption spectrum of the dark-adapted 13-I-bR regenerated with the all-*trans* isomer of 13-iodoretinal is shown in Fig. 2. The absorption maximum was 598 nm.

The absorption spectra of the dark-adapted and the illuminated ($\lambda > 560$ nm, 2 min) 13-I-bR indicated no significant differences, predicting that the all-*trans* isomer is predominant in the dark-adapted 13-I-bR. Chromophores were then extracted from the dark-adapted and the illuminated 13-I-bR, respectively, followed by analysis of the isomer composition by HPLC. Results are presented in Table 1; 97% of the chromophore was an all-*trans* isomer in both specimens.

When the 13-*cis* isomer was added to apomembranes, the regeneration rate was slow and the absorbance peaks around 440 and 500 nm other than 598 nm were observed in the

TABLE 1 Chromophore compositions of 13-I-bR in the dark or illuminated- state

	Dark-Adapted	Illuminated	
		RT*	LT†
All-*trans*	97	97	25
13-*cis*	3	3	75

*Room temperature ($\lambda > 560$ nm, 2 min).
†Dry ice-methanol temperature ($\lambda > 600$ nm, 20 min).

early stages of regeneration (for example, 10 min after addition). After standing overnight, however, only the pigment with $\lambda_{max} = 598$ nm formed and almost all-*trans* isomer was contained. In the case of the addition of 9-*cis* isomer, the 598-nm pigment did not regenerate.

The extinction coefficient of 13-I-bR was estimated by comparing the absorbance maximum of 13-I-bR with that of the native bR. Assuming the extinction coefficient of 54,000 M^{-1} cm^{-1} for the dark-adapted native bR (Tu et al., 1981), the extinction coefficient of 13-I-bR was 58,000 M^{-1} cm^{-1}. The absorption maximum of the protonated Schiff base of 13-iodoretinal with ethanolamine was ~470 nm. The opsin shift of 13-I-bR was ~4600 cm^{-1}.

CD spectrum

Fig. 3 shows the CD spectrum of 13-I-PM and R-PM. In the visible region, the negative and positive bands due to the coupling were observed at 635 and 555 nm respectively, like the native PM. Dissymmetry between the negative band and the positive one was smaller in 13-I-PM than R-PM. The magnitude of the coupling peaks increased in 13-I-PM. The small positive bands were observed around 370 nm in both specimens, suggesting the residual retinaloxime. As seen in Fig. 3 *b*, the CD spectrum of 13-I-bR in the near-UV region showed the negative band around 326 nm and the positive one around 265 nm, respectively. These bands could be attributed to the transitions of the π-electron of the chromophore because they were positioned at longer wavelengths than those of the native bR, in agreement with the shift of visible absorption maximum, and disappeared by bleaching. Three bands originated from aromatic amino acids were observed around 290 nm. The main band at 290 nm was higher in 13-I-bR than R-bR, and subsidiary bands at 285 nm and 295 nm became prominent in 13-I-bR. Thus, replacement of the C-13 methyl group by a bulky iodine atom might cause the increase of steric repulsions with aromatic groups in the van der Waals contacts.

Flash photolysis and proton pumping

The time-resolved absorption spectra of 13-I-bR have shown the formation of the M intermediate with maximum absorbance change at 426 nm and the O intermediate around

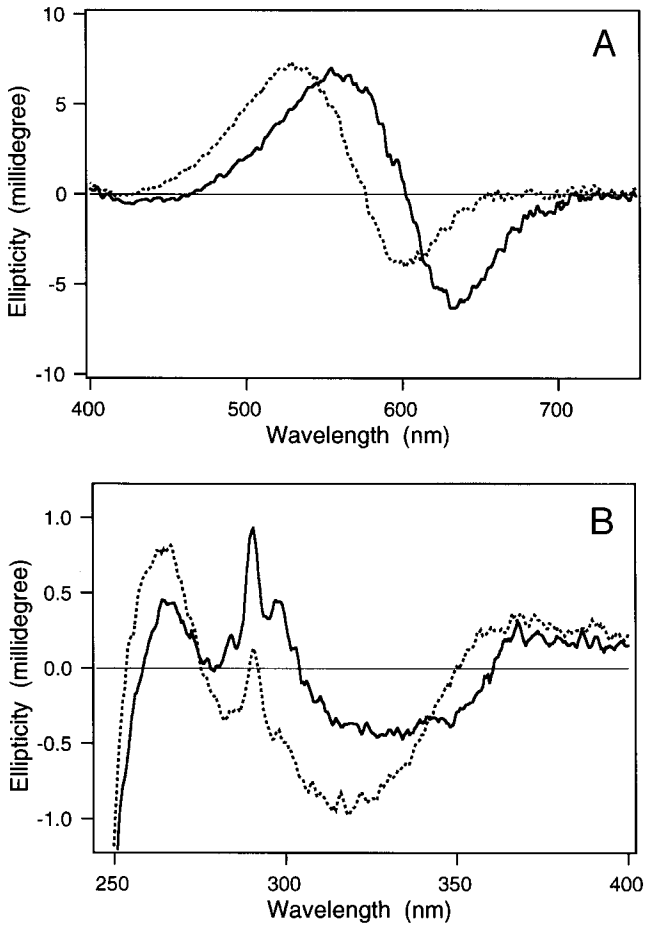

FIGURE 3 CD spectra of R-PM (*dotted line*) and 13-I-PM (*solid line*), in the visible region (*A*) and the near-UV region (*B*).

690 nm. As shown in Table 2, the rise and the decay of the M intermediate of 13-I-bR was slightly faster than the native bR.

Fig. 4 presents transient absorbance changes of 13-I-bR and R-bR. Time constants of M and O decays and the recovery to the ground states are summarized in Table 3. Rise of the M intermediate of 13-I-bR occurred faster than those of R-bR and the native bR.

Next, the light-induced proton pumping activity was investigated. The suspension of 13-I-PM containing the pH indicator dye pyranine was illuminated by a flash (532 nm, 5 ns) at pH 6.5 and 6.8. Fig. 5 *A* shows the results. The light-induced proton release and reuptake similar to the native bR were observed in 13-I-bR, suggesting that 13-

TABLE 2 Time constants of M formation and decay at pH 6.5 (25°C)

	Native bR	13-I-bR
Rise (μs)	53.8	39.7
Decay (ms)	2.41	1.55

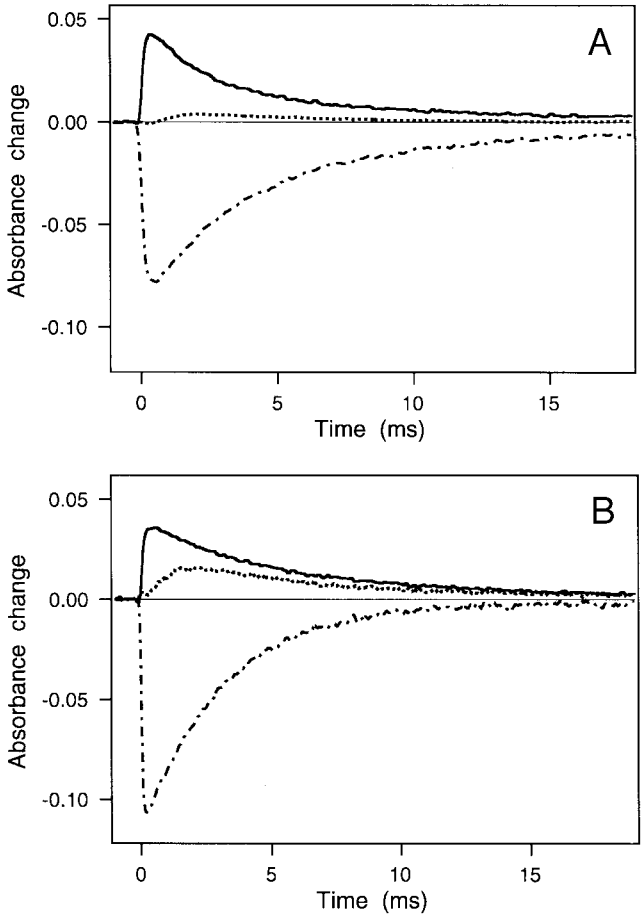

FIGURE 4 (*A*) Transient changes in absorbance of 13-I-bR to follow decay of the M intermediate (*solid line*, measured at 420 nm), the O intermediate (*dotted line*, measured at 710 nm), and the recovery to the ground state (*dash-dotted line*, measured at 570 nm). (*B*) Transient changes in absorbance of R-bR showing kinetics of the M intermediate (*solid line*, measured at 420 nm), the O intermediate (*dotted line*, measured at 660 nm), and the recovery to the ground state (*dash-dotted line*, measured at 550 nm). The measurements were performed on membrane suspensions in 100 mM KCl with 20 mM bis-Tris buffer (pH 6.5) at 20°C.

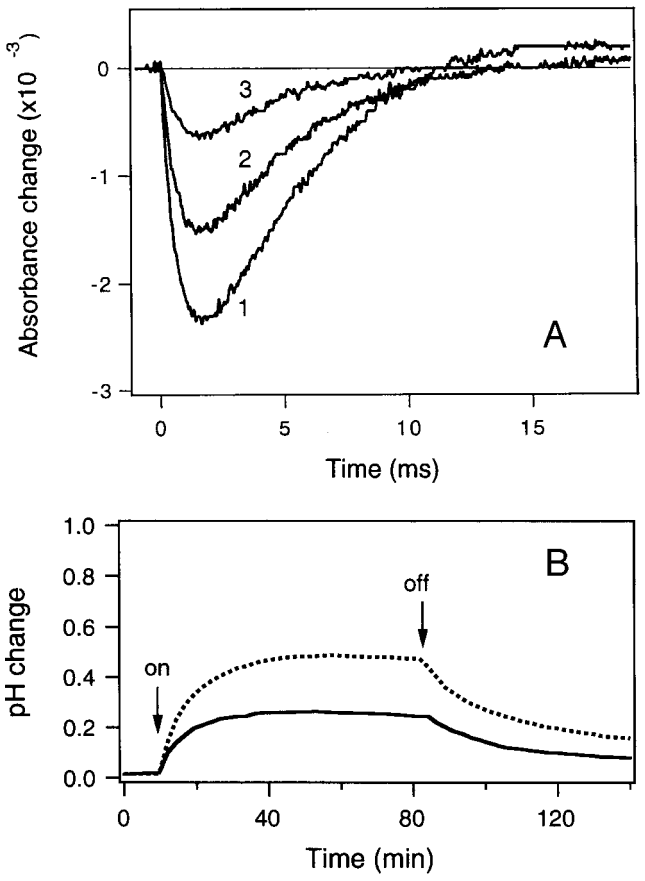

FIGURE 5 (*A*) Light-induced pH changes of membrane suspensions after a laser flash (532 nm, 5 ns) monitored with pyranine are shown for 13-I-bR at pH 6.8 (2) and at pH 6.5 (3) and the native bR at pH 6.8 (1). Transient absorbance changes were measured at 457 nm and at 25°C. (*B*) Light-induced pH changes of the suspensions of 13-I-bR vesicles (*solid line*) and the native bR vesicles (*dotted line*). pH was monitored with a pH electrode at ~25°C.

I-bR underwent the light-driven proton pump through the same intermediates of photocycle as in the native bR. A maximal change in absorbance appeared at 1.7 ms (pH 6.5) and 1.6 ms (pH 6.8) after a flash for 13-I-bR, and 1.8 ms (pH 6.5) and 1.7 ms (pH 6.8) for the native bR. Differences of the rate between 13-I-bR and the native bR correspond to the change in the time course of the photocycle, which may be induced by the alteration of protein-chromophore interactions due to replacing the C-13 methyl group of retinal with iodine.

TABLE 3 Time constants (τ) of M decay, O decay, and recovery to the ground state derived from time courses shown in Fig. 4

	τ (ms)
R-bR	
M decay (420 nm)	4.9
O decay (660 nm)	12.2
Recovery (550 nm)	7.7
13-I-bR	
M decay (420 nm)	2.8
O decay (710 nm)	5.7
Recovery (570 nm)	4.0

After correction for the differences in the absorbance at the wavelength of illumination, the concentration of the specimen and the light scattering of the suspension, the proton pumping activity of 13-I-bR at pH 6.8 became comparable with that of the native bR. At pH 6.5, the yield of the proton pump of 13-I-bR gave ~60% of the native bR. As long as a low light intensity is used, the initial rate of light-induced proton release is constant and maximum in the pH range 3.5–9.0 for the native bR (Kouyama and Nasuda-Kouyama, 1989). The range in which the proton pumping activity becomes constant and maximum would be shifted to the higher pH in the 13-I-bR than the native bR.

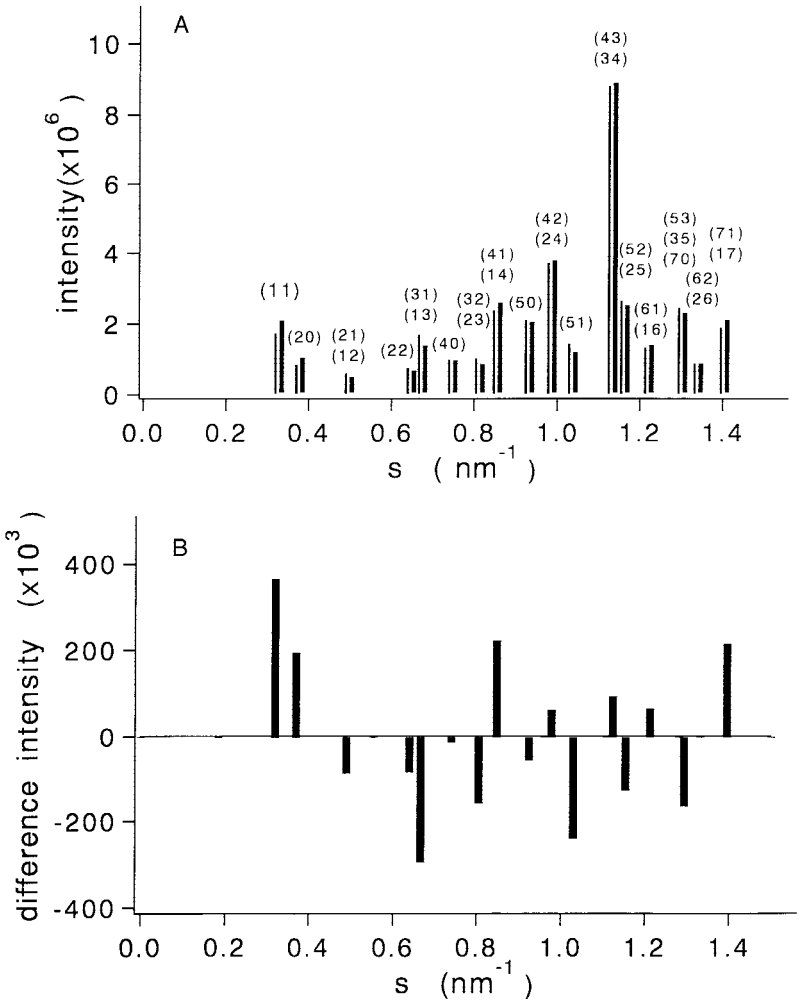

FIGURE 6 (*A*) Diffraction intensities of 13-I-PM (*thick line*) and the native PM (*thin line*). Figures in parentheses represent (h, k) indices of reflections overlapped in each powder line due to the same $h^2 + hk + k^2$ value. (*B*) Difference intensities; (intensity of 13-I-PM) − (intensity of native PM).

The above experiment using pyranine does not necessarily indicate the proton pumping activity because the proton release and uptake can occur from the same protein side. Therefore, the light-induced pH change was also measured with the suspension of the vesicles containing 13-I-bR or the native bR. Results are shown in Fig. 5 *B*. Vesicles containing 13-I-bR showed the same light-induced pH change as the native bR vesicles. It took over 10 min for the pH change to return to the nearly stationary state after light-on or light-off. This indicates that the light-induced pH change is really due to the proton pumping activity, and not to the proton release and uptake from the same protein side.

The M photointermediate of 13-I-bR was trapped at −74°C and its chromophore was extracted at −40°C, followed by the composition analysis by HPLC. Results are shown in Table 1. The chromophore composition before illumination was all-*trans*/13-*cis* = 97:3. This ratio changed to all-*trans*/13-*cis* = 25:75 in the photointermediate. By the same condition, all-*trans*/13-*cis* = 15:85 was obtained in the native photointermediate. These results clearly show that the chromophore of 13-I-bR isomerizes during the photocycle.

X-ray diffraction

X-ray diffraction intensities of 13-I-PM and the native PM are compared in Fig. 6 *A*. Fig. 6 *B* shows the difference between them. In these data, the parameter n in Eq. 1 was 1.83 for 13-I-PM and 1.98 for the native PM. The projection difference density map was computed using difference amplitudes between 13-I-PM and the native PM with phase angles by electron microscopy study (Henderson et al., 1986). The result is shown in Fig. 7 *A*. The error produced in a Fourier synthesis by the error of observed intensities (Blundell and Johnson, 1976) was ~50% of one contour level in Fig. 7 *A*. The position of the main peak (*(1)) was (0.32, 0.08) in fractional coordinates.

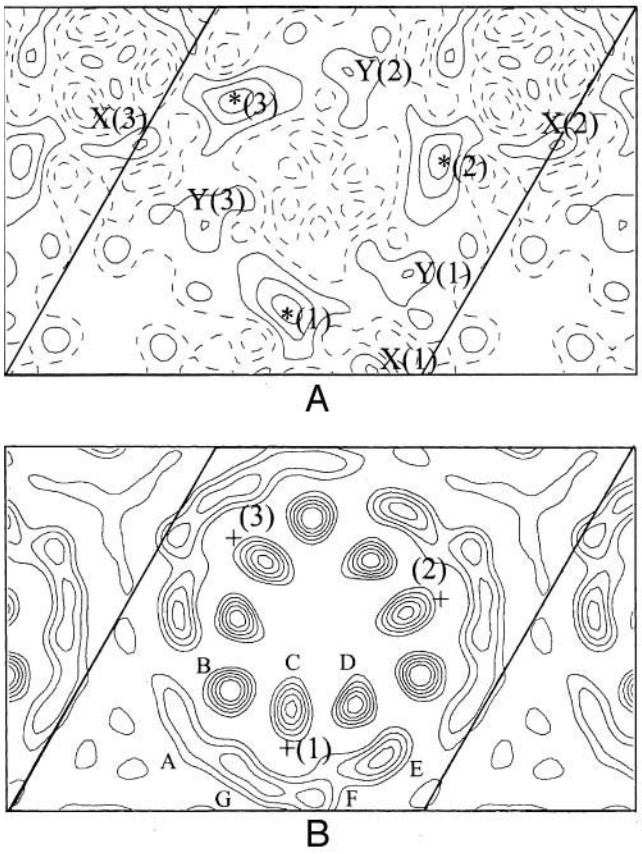

FIGURE 7 (*A*) Projected difference density map between the 13-I-PM and the native PM, which was calculated using the phase angles and the splitting ratios for overlapping reflections obtained by electron microscopy (Henderson et al., 1986). The solid line is the positive level and the dashed line represents 0 or the negative level. The main peak (*(1) ~ *(3)) and subpeaks (X(1) ~ X(3), Y(1) ~ Y(3)) are marked. (*B*) The refined positions of iodine label (+(1) ~ +(3)) superimposed on the projected density map of the native PM. A–G denote the projected seven α-helices of one bR molecule. The N-terminus is in helix A, and the C-terminus is in helix G.

Fig. 7 *B* shows the refined positions of iodine (+(1) − +(3)) superimposed on the projected density map of the native PM. The refined position (+(1)) was (0.33, 0.08), indicating that labeled iodine was located in the vicinity of helix C. Then, the *R* factor (Eq. 3) was 34.2%. The parameter *a* in Eq. 2, denoting occupancy of iodine, was 0.93. The parameter *b* in Eq. 3 was 1.01. This means that intensities of 13-I-PM and the native PM were well scaled. The location of iodine label on the projection map was also calculated based on atomic coordinates of the native bR in the Protein Data Bank (2BRD). When the methyl group bound to C-13 of retinal is replaced by an iodine atom, it is expected to locate at (0.32, 0.07) in fractional coordinates with an I-(C-13) distance of 0.214 nm, and its position is consistent with the observed one.

Several subsidiary peaks and the broadening of the main peak were observed in Fig. 7 *A*. Because the error induced by the error of the observed intensities was only 50% of one contour level in Fig. 7 *A*, the subpeaks were above the average noise level. Similar features were also seen in the difference density map of 13-Br-PM by Büldt et al. (1991). When the iodine atom was assumed to be located at each position of the subpeaks in Fig. 7 *A* (X(1)–X(3), Y(1)–Y(3)) with various occupancies, the *R* factor (Eq. 3) was always >80%. This suggested that subpeaks did not indicate real locations of iodine atoms. To clarify the origins of them, the effect of the use of phases and splitting ratios for overlapped reflections from the native PM on the difference Fourier map was examined by model calculations. The structure factor of the iodine-labeled PM model was constructed from the structure factor of the native PM and the atomic scattering factor of iodine located in the refined position (Eq. 2). The intensities of powder lines were derived by summing reflections with the same value of $h^2 + hk + k^2$.

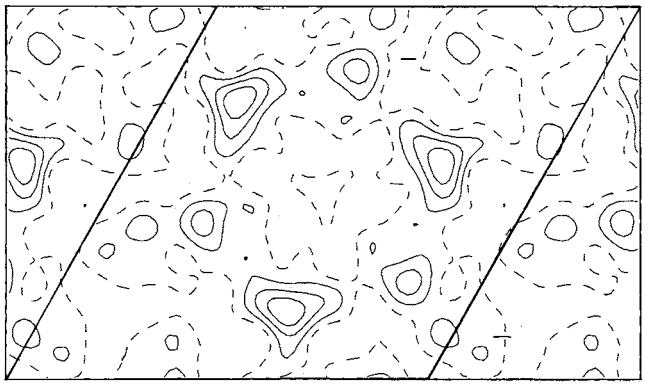

FIGURE 8 Model calculation. The difference projection density map was calculated from the difference amplitudes between the iodine-labeled PM model and the native PM, with phase angles of the native PM obtained by electron microscopy. Overlapped intensities of both the iodine-labeled PM model and the native PM were separated using the intensity ratios of electron microscopic data. Dashed lines depict 0 level. Negative levels were omitted. Contour lines were drawn for the 0.2 level.

In model calculations, both overlapped intensities of the iodine-labeled PM model and the native PM were separated using the intensity ratios of electron microscopic data (Henderson et al., 1986) and the structure factor amplitude of each (*h*, *k*) reflection was derived as the square root of each intensity. The projection difference density map was calculated from difference amplitudes between them with phase angles of the native PM derived by electron microscopy. As shown in Fig. 8, the broadening of the main peak and several subpeaks similar to those in Fig. 7 *A* were regained. Thus, the present analyses lead to the suggestion that the broadening of the main peak and the appearance of subpeaks in Fig. 7 *A* were mainly caused by neglecting the changes in phase angles of the structure factor inherent in a heavy atom substitution, and that no significant structural change occurred by the replacement of the C-13 methyl group with iodine in parallel to the membrane plane. Detailed model calculations will be reported elsewhere.

DISCUSSION

The x-ray diffraction pattern showed that 13-I-PM retained the crystalline structure with the same lattice constant as the native PM. Also, the visible CD showed a biphasic band, and thus indicated the exciton coupling between bR within the trimer, like the native PM. To determine the structural change induced by replacement of the 13-methyl group of the native retinal with iodine atoms, accurate x-ray diffraction intensity was needed. The oriented membrane specimen is preferable to obtain the high S/N intensity data. However, as the membrane sample oriented by dehydration has always some disorientation, that is, mosaicity, the Lorentz correction must be carefully done. In this study, the Lorentz factor was determined by comparing the intensities with those from the membrane suspensions in which s^2 could be properly used. The main positive peak in the difference Fourier map between 13-I-PM and the native PM suggested the position of iodine atoms, but in the difference projection map (Fig. 7 *A*), the main peak was broad and secondary peaks were observed within bR molecules. The model calculation showed that the broadening of the main peak and the appearance of secondary peaks happened mainly due to the application of the phases from the native PM to 13-I-PM. However, the broadening of the main peak is not prominent in 9-Br-PM (Büldt et al., 1991). The sum of the squares of phase angle differences between the halogen-labeled PM model and the native PM was 201.9 for 9-Br-PM and 1470 for 13-I-PM. Thus, the broadening of the main peak and the appearance of secondary peaks in 13-I-PM are consistent with the larger difference of phase angles from the native ones than 9-Br-PM. Therefore, the difference projection map derived in this study implies that the change of the bacterioopsin structure that should be caused by the replacement of the 13-methyl group of retinal with a heavy atom is not seen in the difference projection map, and appears to take place in the normal direction to the membrane plane. The position of iodine determined by the difference Fourier synthesis agreed with the calculated one based on the 3D structure by electron microscopy (Grigorieff et al., 1996).

In the calculation, the position of iodine was estimated by extending the bond from C(13)-CH_3 (0.150 nm) to C(13)-I (0.214 nm) without rotating the chromophore plane. It resulted that the iodine atom should shift by 0.04 nm normally from the position of the 13-methyl group. To get rid of the further steric hindrance between 13-I and the surrounding residues by tilting the retinal, it is needed for its conjugated plane to rotate ~20°. This rotation would induce the shift of the iodine atom by ~0.1 nm from the 13-methyl group site of the native bR in parallel to the membrane plane. Thus the x-ray diffraction study suggested that retinal might move along the normal to the membrane plane without tilting its conjugated plane by replacing 13-methyl group with iodine.

As the opsin shift of 13-I-bR is identical to that of the native bR, the electrostatic interaction between the π-electron of 13-iodoretinal and residues in the retinal binding pocket changes little by the replacement of 13-methyl group with iodine, but the near-UV CD spectra showed that there were large reductions in the 317-nm band and the 260-nm band by the replacement. It has been suggested that the CD bands in this region arise from dissymmetric interaction between retinal and opsin and provide information concerning tertiary structural changes of the protein (Becher and Cassim, 1976). Also, the CD in 290-nm band increased and the side bands at 285 nm and 295 nm appeared prominently in 13-I-bR. As these CD bands are attributed to the transitions of aromatic amino acids tryptophan, tyrosine, and phenylalanine (Becher and Cassim, 1976), the present data might indicate that the steric interaction between the retinal and aromatic groups became stronger by replacing the 13-methyl group with iodine. HPLC has shown that 13-I-bR contained almost 100% all-*trans* isomer in the dark and did no light-dark adaptation. This result could also be explained by the increase of the steric interaction between retinal and residues in the retinal binding pocket, due to the replacement of the 13-methyl group with a heavy atom. Gärtner et al. (1983) reported that the retinal analog with absence of the methyl group at C-13, 13-desmethylretinal, leads to a predominant formation of the 13-*cis* isomer (85%) in the regenerated pigment. For the native bR, the recent estimates are that the ratio of all-*trans* to 13-*cis* is 2:1 (Ebrey, 1993). In 13-I-bR, the contacts between a bulky atom at the 13-methyl site and residues such as Trp-182 and Leu-93 must increase steric repulsions and push 13-iodoretinal into the extracellular side. As a result, the retinal binding pocket would be unable to accommodate the 13-*cis* conformation, which needs larger space around Schiff base than the all-*trans* conformation. Hashimoto et al. (1997) suggested by UV resonance Raman spectra that there is a steric interaction between the 13-methyl group and Trp-182 in even the native bR. The change of the CD band in the 250–350 nm region may provide the evidence that 13-iodoretinal increases steric interaction with Trp-182 and/or Trp-86, positioned at the opposite side from retinal. It is also suggested by this consideration that structural changes of retinal and opsin by replacing the 13-methyl group with iodine occurred in the direction of the membrane normal. This is consistent with the result derived by x-ray, in which no significant structural change was observed in parallel to the membrane plane.

Flash photolysis showed that the 13-I-bR underwent similar late steps of the photocycle and proton pump activity to those of the native bR. Both rise and decay of the M-intermediate and the concomitant proton release occurred slightly faster than the native bR. Because 13-I-bR shows almost 100% all-*trans* conformation in the dark and no light-dark adaptation, a question may arise whether the all-*trans* to 13-*cis* isomerization took place during the pho-

tocycle. By examining isomer compositions of the M-like intermediate trapped at −74°C, it was confirmed that the 13-*cis* isomer increased from 3% to 75% after light illumination of 13-I-bR. This experiment clearly indicates that 13-I-bR performed the all-*trans* to 13-*cis* isomerization during the photocycle. These facts support a statement that the all-*trans* to 13-*cis* photoisomerization is essential for the photochemical transformation and function of bR (Fang et al., 1983; Kölling et al., 1984; Chang et al., 1985).

The decay of the O-intermediate and the recovery to the ground state of 13-I-bR were significantly faster than the native bR. There is evidence that the van der Waals interactions between the 9-methyl group and the 13-methyl group of retinal and the surrounding residues play a important role in the decay of the O-intermediate. Weidlich et al. (1996) reported that the steric interaction between the 9-methyl group of retinal and Trp-182 controls 13-*cis* to all-*trans* reisomerization and proton uptake in the photocycle. Gärtner et al. (1983) showed that the replacement of the methyl group at C-13 by a hydrogen atom leads to a predominant formation of the 13-*cis* isomer (85%) and the M-intermediate decays five times slower than the native bR, but bRs containing 13-ethylretinal and 13-n-propylretinal increase the ratio of the all-*trans* isomer to 67% and 50%, respectively, and the decay times of M-intermediates are similar to the native one. However, Delaney et al. (1997) describes that the decay of the O-intermediate is greatly slowed upon replacement of Leu-93, a residue in van der Waals contact with retinal, by less bulky amino acids Ala or Thr, but is accelerated to a rate similar to that seen in the native bR by exchange of the native retinal in the Leu-93→Ala mutant with the 9,11-bridged or 11,13-bridged retinal analogs. They also concluded that the protein-induced restriction of the conformational flexibility in retinal is a key structural requirement for the efficient protein-retinal coupling in the bR photocycle. Also in 13-I-bR, as the 13-methyl group is replaced by a more bulky atom, the O-intermediate may well decay faster than the native bR due to the increased steric repulsion between 13-I and the surrounding residues.

We thank Dr. T. Nakagawa for using computer programs to process x-ray diffraction intensities recorded on the image plate and calculating integrated intensity by curve-fitting.

REFERENCES

Becher, B., and J. Y. Cassim. 1976. Effects of light adaptation on the purple membrane structure of *Halobacterium halobium*. *Biophys. J.* 16:1183–1201.

Blundell, T. L., and L. N. Johnson. 1976. Protein Crystallography. Academic Press, London. 409–411.

Büldt, G., K. Konno, K. Nakanishi, H.-J. Plöhn, B. N. Rao, and N. A. Dencher. 1991. Heavy atom-labeled retinal analogs located in bacteriorhodopsin by x-ray diffraction. *Photochem. Photobiol.* 54:873–879.

Cao, Y., G. Váró, A. L. Klinger, D. M. Czajkowsky, M. S. Braiman, R. Needleman, and K. Lanyi. 1993. Proton transfer from Asp-96 to the bacteriorhodopsin Schiff base is caused by a decrease of the pKa of Asp-96, which follows a protein backbone conformational change. *Biochemistry.* 32:1981–1990.

Chang, C. H., R. Govindjee, T. G. Ebrey, T. A. Bagley, G. Dollinger, L. Eisenstein, J. Marque, H. Roder, J. Vittitow, and J. M. Fang. 1985. *Trans*/13-*cis* isomerization is essential for both the photocycle and proton pumping of bacteriorhodopsin. *Biophys. J.* 47:509–512.

Delaney, J. K., G. Yahalom, M. Sheves, and S. Subramaniam. 1997. Reducing the flexibility of retinal restores a wild-type-like photocycle in bacteriorhodopsin mutants defective in protein-retinal coupling. *Proc. Natl. Acad. Sci. U.S.A.* 94:5028–5033.

Dencher, N. A., P. A. Burghaus, and S. Grzesiek. 1986. Determination of the net proton-hydroxide ion permeability across vesicular lipid bilayers and membrane proteins by optical probes. *Methods Enzymol.* 127: 746–760.

Ebrey, T. G. 1993. Light energy transduction in bacteriorhodopsin. *In* Thermodynamics of Membrane Receptors and Channels. M. B. Jackson, editor. CRC Press Inc., Boca Raton, FL. 353–387.

Edman, K., P. Nollert, A. Royant, H. Belrhall, E. Pebay-Peyroula, J. Hajdu, R. Neutze, and E. M. Landau. 1999. High-resolution x-ray structure of an early intermediate in the bacteriorhodopsin photocycle. *Nature.* 401: 822–826.

Fang, J.-M., J. D. Carriker, V. Balogh-Nair, and K. Nakanishi. 1983. Evidence for the necessity of double bond (13-Ene) isomerization in the proton pumping of bacteriorhodopsin. *J. Am. Chem. Soc.* 105: 5162–5164.

Gärtner, W., P. Towner, H. Hopf, and D. Oesterhelt. 1983. Removal of methyl groups from retinal controls the activity of bacteriorhodopsin. *Biochemistry.* 22:2637–2644.

Govindjee, R., Z. Dancshazy, T. G. Ebrey, C. Longstaff, and R. R. Rando. 1988. Photochemistry of monomethylated and permethylated bacteriorhodopsin. *Biophys. J.* 54:557–562.

Grigorieff, N., T. A. Ceska, K. H. Downing, J. M. Baldwin, and R. Henderson. 1996. Electron-crystallographic refinement of the structure of bacteriorhodopsin. *J. Mol. Biol.* 259:393–421.

Grzesiek, S., and N. A. Dencher. 1986. Time-course and stoichiometry of light-induced proton release and uptake during the photocycle of bacteriorhodopsin. *FEBS Lett.* 127:746–760.

Hamanaka, T., K. Hiraki, and T. Mitsui. 1982. X-ray diffraction studies of purple membranes reconstituted from brown membrane. *Methods Enzymol.* 88:268–271.

Hashimoto, S., K. Obata, H. Takeuchi, R. Needleman, and J. K. Lanyi. 1997. Ultraviolet resonance Raman spectra of Trp-182 and Trp-189 in bacteriorhodopsin: novel information on the structure of Trp-182 and its steric interaction with retinal. *Biochemistry.* 36:11583–11590.

Henderson, R., J. M. Baldwin, K. H. Downing, J. Lepault, and F. Zemlin. 1986. Structure of purple membrane from *Halobacterium halobium*: recording, measurement and evaluation of electron micrographs at 3.5 Å resolution. *Ultramicroscopy.* 19:147–178.

Hiraki, K., T. Hamanaka, K. Yoshihara, and Y. Kito. 1987. Bacteriorhodopsin analogs regenerated with enantiomers of 5,6-epoxyretinal. *Biochim. Biophys. Acta.* 891:177–193.

Humphrey, W., I. Logunov, K. Schulten, and M. Sheves. 1994. Molecular dynamics study of bacteriorhodopsin and artificial pigments. *Biochemistry.* 33:3668–3678.

Jubb, J. S., D. L. Worcester, H. L. Crespi, and G. Zaccai. 1984. Retinal location in purple membrane of *Halobacterium halobium*: a neutron diffraction study of membranes labeled in vivo with deuterated retinal. *EMBO J.* 3:1455–1461.

Katre, N. V., P. K. Wolber, W. Stoeckenius, and R. M. Stroud. 1981. Attachment site(s) of retinal in bacteriorhodopsin. *Proc. Natl. Acad. Sci. U.S.A.* 78:4068–4072.

Kimura, Y., D. G. Vassylyev, A. Miyazawa, A. Kidera, M. Matsushima, K. Mitsuoka, K. Murata, T. Hirai, and Y. Fujiyoshi. 1997. Surface of bacteriorhodopsin revealed by high-resolution electron crystallography. *Nature.* 389:206–211.

Kölling, E., W. Gärtner, D. Oesterhelt, and L. Ernst. 1984. Sterically fixed retinal-analog prevents proton-pumping activity in bacteriorhodopsin. *Angew. Chem. Int. Ed. Engl.* 23:81–82.

Kouyama, T., and A. Nasuda-Kouyama. 1989. Turnover rate of the proton pumping cycle of bacteriorhodopsin: pH and light-intensity dependence. *Biochemistry.* 28:5963–5970.

Lanyi, J. K. 1993. Proton translocation mechanism and energetics in the light-driven pump bacteriorhodopsin. *Biochim. Biophys. Acta.* 1183: 241–261.

Luecke, H., B. Schobert, H.-T. Richter, J.-P. Cartailler, and J. K. Lanyi. 1999a. Structure of bacteriorhodopsin at 1.55 Å resolution. *J. Mol. Biol.* 291:899–911.

Luecke, H., B. Schobert, H.-T. Richter, J.-P. Cartailler, and J. K. Lanyi. 1999b. Structural changes in bacteriorhodopsin during ion transport at 2 angstrom resolution. *Science.* 286:255–261.

Oesterhelt, D., and W. Stoeckenius. 1974. Isolation of the cell membrane of *Halobacterium halobium* and its fractionation into red and purple membrane. *Methods Enzymol.* 31:667–678.

Oesterhelt, D., J. Tittor, and E. Bamberg. 1992. A unifying concept for ion translocation by retinal proteins. *J. Bioenerg. Biomembr.* 24:181–191.

Pebay-Peyroula, E., G. Rummel, J. P. Rosenbusch, and E. M. Landau. 1997. X-ray structure of bacteriorhodopsin at 2.5 Å from microcrystals grown in lipidic cubic phases. *Science.* 277:1676–1681.

Racker, E., B. Violand, S. O'Neal, M. Alfonzo, and J. Telford. 1979. Reconstitution, a way of biochemical research; some new approaches to membrane-bound enzymes. *Arch. Biochem. Biophys.* 198:470–477.

Royant, A., K. Edman, T. Ursby, E. Pebay-Peyroula, E. M. Landau, and R. Neutze. 2000. Helix deformation is coupled to vectorial proton transport in the photocycle of bacteriorhodopsin. *Nature.* 406:645–648.

Sass, H. J., G. Büldt, R. Gessenich, D. Hehn, D. Neff, R. Schlesinger, J. Berendzen, and P. Ormos. 2000. Structural alterations for proton translocation in the M state of wild-type bacteriorhodopsin. *Nature.* 406: 649–652.

Stoeckenius, W., and R. A. Bogomolni. 1982. Bacteriorhodopsin and related pigments of halobacteria. *Annu. Rev. Biochem.* 52:587–616.

Subramaniam, S., and R. Henderson. 2000. Molecular mechanism of vectorial proton translocation by bacteriorhodopsin. *Nature.* 406: 653–657.

Subramaniam, S., M. Lindahl, P. Bullough, A. R. Faruqi, J. Tittor, D. Oesterhelt, L. Brown, J. K. Lanyi, and R. Henderson. 1999. Protein conformational changes in the bacteriorhodopsin photocycle. *J. Mol. Biol.* 287:145–161.

Suzuki, T., Y. Fujita, Y. Noda, and S. Miyata. 1986. A simple procedure for the extraction of the native chromophore of visual pigments: the formaldehyde method. *Vision Res.* 26:425–429.

Tu, S. I., D. Shiuan, F. Ramirez, and B. Mckeever. 1981. Effects of fluorescamine modification on light-induced H^+-movement in reconstituted purple membrane of halobacteria. *Biochem. Biophys. Res. Commun.* 99:584–590.

Weidlich, O., B. Schalt, N. Friedman, M. Sheves, J. K. Lanyi, L. S. Brown, and F. Siebert. 1996. Steric interaction between the 9-methyl group of the retinal and tryptophan 182 controls 13-*cis* to all-*trans* reisomerization and proton uptake in the bacteriorhodopsin photocycle. *Biochemistry.* 35:10807–10814.